Journal of Alloys and Compounds 563 (2013) 180–185

Contents lists available at SciVerse ScienceDirect

Journal of Alloys and Compounds

journal homepage: www.elsevier.com/locate/jalcom

Electrochemical testing of laser treated bronze surface

B.S. Yilbas [a,*], Ihsan-ul-Haq Toor [a], Jahanzaib Malik [a], F. Patel [a], C. Karatas [b]

[a] Dept. of Mechanical Engineering, King Fahd University of Petroleum and Minerals (KFUPM), Dhahran 31261, Saudi Arabia
[b] Engineering Faculty, Hacettepe University, Ankara, Turkey

ARTICLE INFO

Article history:
Received 11 November 2012
Received in revised form 9 February 2013
Accepted 14 February 2013
Available online 27 February 2013

Keywords:
Laser melting
Corrosion resistance
Bronze

ABSTRACT

Electrochemical testing of laser treated bronze surface is carried out and corrosion resistance of the surface is assessed. Morphological and metallurgical changes in the laser treated layer are examined using scanning electron microscope, energy dispersive spectroscopy, and X-ray diffraction. The pit sites formed at the surface are analyzed using scanning electron microscope. It is found that laser treatment improves the corrosion resistance of the treated surface. Fine grains are formed in the surface region of the laser treated layer, which are attributed to the large cooling rates from the surface.

1. Introduction

Bronze is a copper alloy and it is widely used in marine environment due to its combination of toughness and resistance to the aqueous corrosion. However, corrosion and erosion take place at the fluid–metal interface and this adverse effect accelerates for the surfaces where the non-uniform microstructures are present. In general grain refining, with uniform microstructures at the surface vicinity of the alloy, improves the corrosion and erosion resistance at the surface. One of the methods to improve the alloy microstructure in the surface vicinity is to introduce control melting incorporating the high power laser beam. In addition, laser treatment of the surfaces is involved with precision of operation, short treatment duration, shallow heat affected zone, and low cost. However, the proper selection of the laser parameters is vital in surface treatment process to avoid the surface asperities because of the excessive heating. The surface asperities such as cavities and micro-cracks act like a defect sites for accelerated corrosion at the surface. Consequently, investigation into laser treatment of bronze surface in relation to corrosion prevention in aqueous solution becomes essential.

Considerable research studies were carried out to examine laser treatment of bronze surfaces. Laser treatment of aluminum bronze was studies by Xu et al. [1]. They demonstrated that the microstructure of the treated surface was cellulated crystals and it became dendritic crystals in the midsection of the treated layer. Laser treating of sintered bronze was investigated by Gisario et al. [2]. They performed thermographic analysis on the treated samples to evaluate the thermal dispersion at the surface. Laser treatment of bronze surface and corrosion resistance was examined by Tang et al. [3]. They showed that the galvanic effect between the laser treated and as-received samples were small, which justified the use of laser surface alloying as a feasible method in the local surface treatment of bronze. The cavitation erosion resistance of laser treated bronze was studies by Kwok et al. [4]. Their findings revealed that the cavitation erosion resistance of the laser treated surface was improved by at most 7.5 times that of as-received bronze surface. In addition, laser treatment enhanced the corrosion resistance of the surface considerably. Electrochemical response of the laser treated bronze surface was examined by Klassen et al. [5]. They illustrated that the oxide formed at the surface during laser treatment behaved as the passivation film improving the corrosion resistance of the surface. The corrosion resistance of laser treated bronze surface was studied by Mazurkevich et al. [6]. They indicated that the laser treatment of the surface improved the corrosion resistance notably. The influence of laser treatment on the surface properties of copper alloys was investigated by Garbacz et al. [7]. They incorporated Raman Spectroscopy to examine the phase composition of the corroded layers at the laser treated surface. The corrosion characteristics of laser treated Ni–Al–Bronze surface were examined by Kawazoe et al. [8]. Their findings revealed that Ni–Al–Bronze had quenching characteristics closely related to that of steel and the corrosion resistance of the surface improved after the laser treatment process. Laser treatment of bronze and titanium alloy was investigated by Kac et al. [9]. They showed that the high chemical homogeneity and fine structure of the melted zone were attributed to high cooling rates due to the short interaction time with Nd:YAG pulsed laser radiation and relatively small volume of the melted

* Corresponding author.
E-mail address: bsyilbas@kfupm.edu.sa (B.S. Yilbas).

0925-8388/$ - see front matter © 2013 Elsevier B.V. All rights reserved.
http://dx.doi.org/10.1016/j.jallcom.2013.02.094

Table 1
Laser heating conditions used in the experiment.

Scanning speed (cm/s)	Power (W)	Frequency (Hz)	Nozzle gap (mm)	Nozzle diameter (mm)	Focus setting (mm)	N_2 pressure (kPa)
10	80	1000	1.5	1.5	127	500

material. Yilbas et al. [10] studied laser treatment of bronze surfaces with the presence of B_4C particles. They demonstrated that the laser treated surface produced was relatively free from defects and asperities with a microhardness that was notably higher than that of the as-received bronze substrate.

Laser surface treatment of bronze was investigated previously [11,12]. The main emphasis in the previous studies was on the improvement of microhardness at the surface and corrosion resistance of the treated surface was left obscure. Consequently, in the present study, laser treatment of aluminum bronze surface is carried out and corrosion resistance of the treated surface is examined incorporating the electrochemical tests in the electrolytic solution. The morphological and microstructural changes in the laser treated layer are examined using scanning electron microscope, energy dispersive spectroscopy, and X-ray diffraction. The pits sites at the surface are also analyzed.

2. Experimental work

The CO_2 laser (LC-ALPHAIII) delivering a nominal output power of 2 kW was used to irradiate the workpiece surface. The focusing lens has focal length of 127 mm and the focused laser beam diameter was about 0.3 mm at the workpiece surface. Nitrogen emerging from the conical nozzle was used as an assisting gas. The various surface treatment tests were carried out incorporating different laser parameters and the laser parameters resulting in crack free surfaces with low surface roughness were selected. The laser treatment conditions are given in Table 1. The laser treatment experiments were repeated three times to ensure the same topology and similar microstructures forming in the treated layer.

The aluminum bronze with elemental composition (wt%) of 9% Al, 3% Fe, and balance of Cu was used in the experiments. The bronze sheet was 3 mm in thickness and the size of the samples used in the experiments was 20 × 20 (length × width) mm.

Corrosion tests (Potentiodynamic polarization, Tafel behavior and electrochemical impedance spectroscopy) were carried out in a three electrode cell, which composed of a specimen as a working electrode, a Pt wire as a counter electrode, and a saturated calomel reference electrode (SCE). The specimens were degreased in benzene, cleaned ultrasonically, and subsequently washed with distilled water prior to electrochemical tests. The investigations were carried out with an exposed working electrode area of 0.07 cm^2 in 0.1 M NaCl solution at room temperature in PCI4/750 Gamry potentiostat and repeated several times to ensure the reproducibility of the data. DC105 corrosion software was used to analyze the Tafel region, while Potentiodynamic polarization experiments were performed at a scan rate of 0.5 mV/s.

Electrochemical impedance spectroscopy (EIS) measurements were carried out at OCP, by applying a sinusoidal potential perturbation of 10 mV with frequency sweep from 100 kHz to 0.01 Hz. The impedance data were analyzed and fitted to appropriate equivalent electrical circuit using the GAMRY framework software.

A Jeol 6460 electron microscopy was used for the SEM examinations and a Bruker D8 Advanced with Cu Kα radiation was used for XRD analysis. A typical setting for the XRD was 40 kV and 30 mA, the scanning angle (2θ) was ranged over 20–80°. The parabolically-shaped Göbel Mirror was used in the Bruker D8 Advanced, which provided highly-parallel X-ray beams.

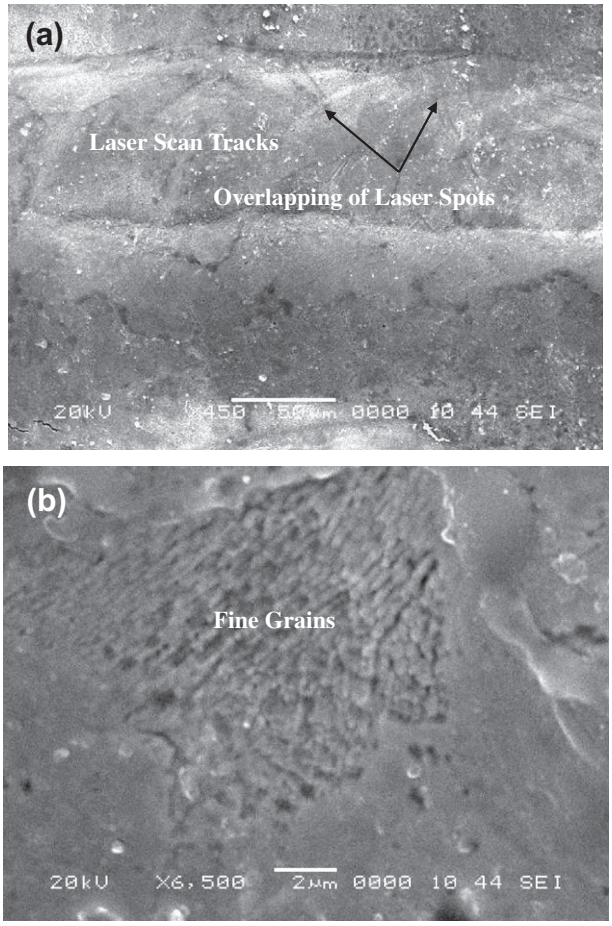

Fig. 1. SEM micrographs of laser treated surface: (a) laser scanning tracks and overlapping of irradiated spots, and (b) fine grains at the surface.

3. Results and discussion

Potentiodynamic response of laser treated bronze surface is investigated. Microstructural and morphological changes in the laser treated layer are examined prior and after the electrochemical tests.

Fig. 1 shows SEM micrographs of laser treated surface prior to the electrochemical tests. The surface comprises of regular laser scan tracks, which are equally spaced at the surface. Since the laser power intensity was adjusted to avoid evaporation at the surface, no laser induced cavity is formed at the surface. In addition, no micro-cracks or some other surface asperities are visible. It should be noted that the thermal conductivity of bronze is high; consequently, conduction heat transfer from surface region to the solid bulk is high. This, in turn, suppresses the development of high temperature gradients and high stress levels in the surface region.

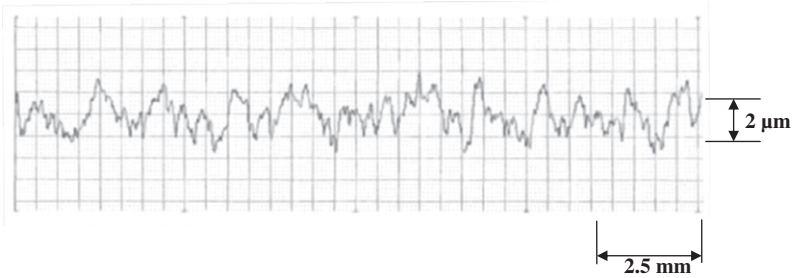

Fig. 2. Surface roughness chart for laser treated surface.

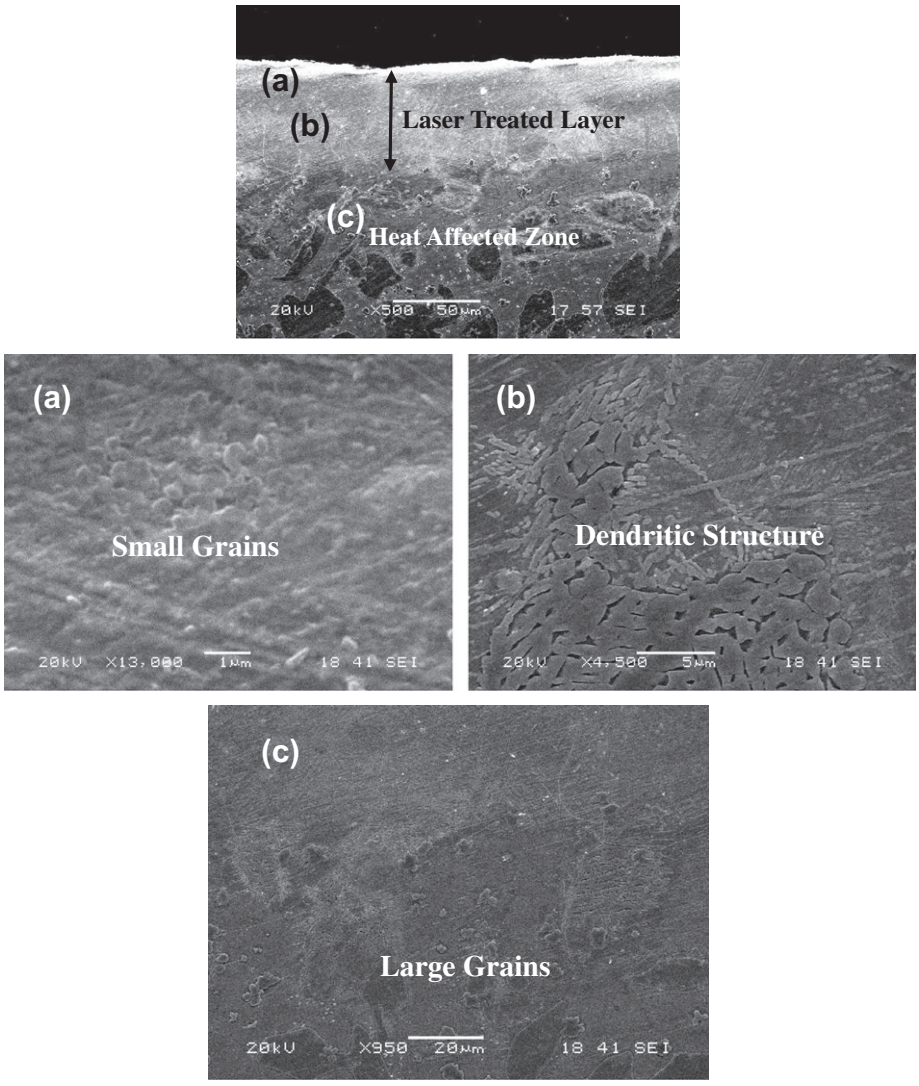

Fig. 3. SEM micrographs of cross-section of laser treated layer: (a) small grains in the surface region, (b) dendritic structure in mid-thickness of treated layer, (c) large grains at interface.

Table 2
EDS data and corresponding locations at the laser treated surface (wt%).

Spectrum	N	Al	Fe	Cu
Spectrum 1	4.2	8.9	2.9	Balance
Spectrum 2	4.1	8.7	2.8	Balance
Spectrum 3	3.6	8.4	3.0	Balance
Spectrum 4	3.9	8.6	2.7	Balance

Hence, thermally induced micro-cracks do not form at the surface. The close examination of the surface reveals the overlapping of irradiated laser spots along the scanning tracks. The overlapping ratio is of the order of 70%, which enables the continuous melting of the substrate along the scanning directions at the surface. Although presence of overlapping of irradiated spots increases the surface roughness, the roughness of the treated surface is in the order of 2 μm as evident from Fig. 2, in which the surface roughness chart is shown. Since nitrogen is used as an assisting gas during the laser treatment process, the surface color changes from bright brown to mahogany, which indicates the formation of Cu_3N compound at the surface during the treatment process. The presence of small grains at the surface suggests that the dissolution of Cu_3N takes place in the surface region due to the high temperature, which is also observed in the previous study [11]. It should be noted that high cooling rates at the surface contributes significantly to the formation of fine grains at the surface while enhancing the microhardness as consistent with the previous findings [11].

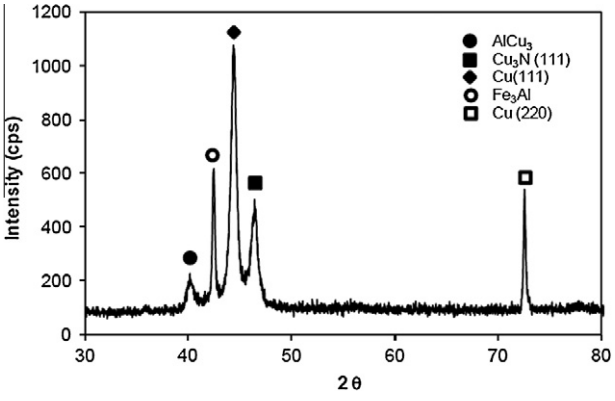

Fig. 4. X-ray diffractogram of laser treated surface.

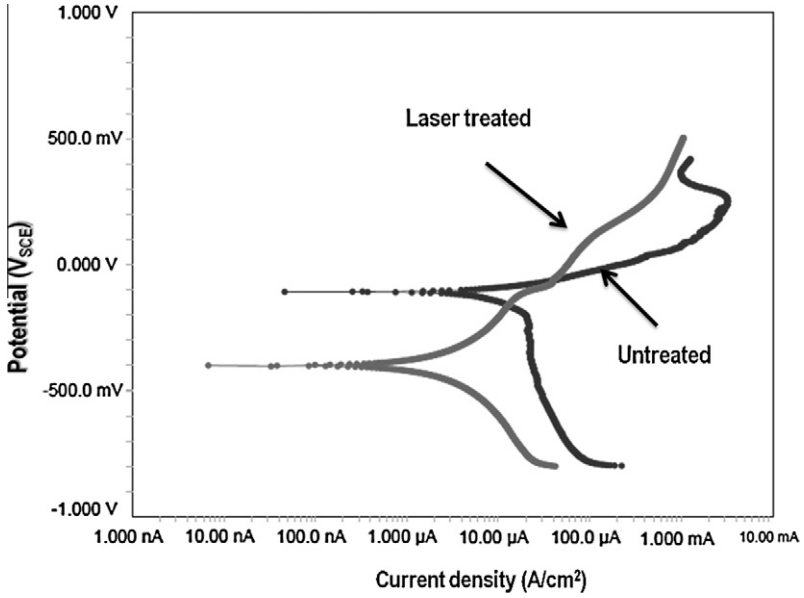

Fig. 5. Potentiodynamic polarization response of laser treated and untreated specimens in 0.1 M NaCl solution.

Table 3
Results of electrochemical tests for laser treated and untreated alloy in 0.1 M NaCl solution.

	E_{corr} (mV_{SCE})	i_{corr} (nA)	i_p (µA)	E_{Pit} (mV_{SCE})
Laser treated	−400	10	10	330
Untreated	−120	100	300	70

Fig. 3 shows SEM micrographs of the cross-section of the laser treated layer. The treated layer extends uniformly below the surface. The thickness of the treated layer is on the order of 40 µm. It is evident that no large scale defects including major cracks are observed across the cross-section of the treated layer. Laser treated layer consists of mainly three regions. Fine grains forming dense layer are present in the first region. The formation of the fine grains is attributed to the high cooling rates at the surface of the treated layer. It should be noted that the convective cooling of the assisting gas contributes considerably to the high cooling rates at the surface. In addition, formation of Cu_3N compound at the surface results in the volume shrinkage in the surface vicinity, which in turn contributes to the formation of the dense layer in the surface region. Although high cooling rates results in high temperature gradients and thermal stresses in the surface region, no microcracks or crack-network is observed. This is attributed to the self-annealing effect of the initially formed laser scanning tracks. It should be noted that laser scans the surface along the tracks during the treatment process. Initially formed tracks cools slowly because of the heat transfer from the recently formed scan tracks. Table 2 gives the EDS data at the surface after the laser treatment process. Elemental composition remains almost uniform after the laser treatment process. Although the quantification of light elements is involved with error in the EDS data, the presence of

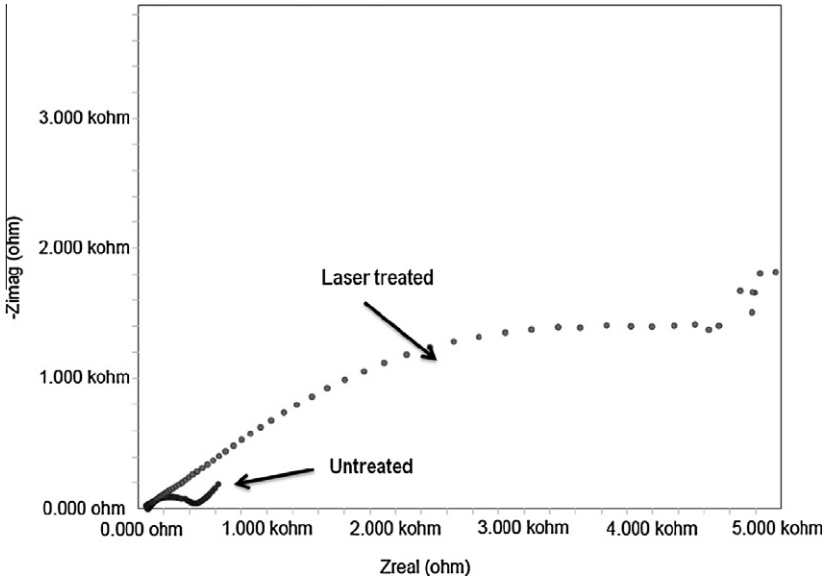

Fig. 6. EIS response of laser treated and untreated specimens in 0.1 M NaCl solution.

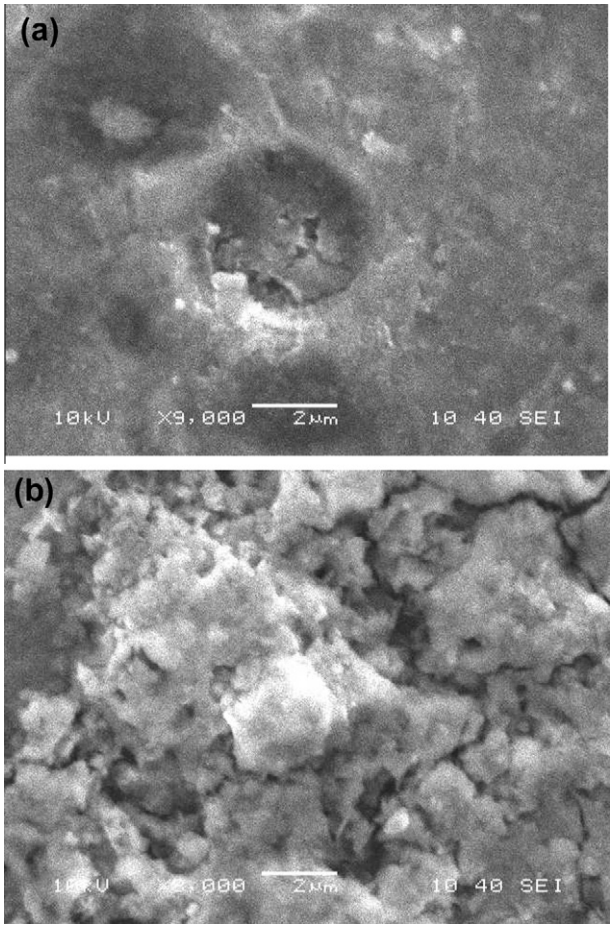

Fig. 7. SEM micrographs of laser pit sites after electrochemical tests: (a) laser treated surface, and (b) as-received surface.

nitrogen is evident from Table 2 indicating the formation of the nitride compound at the surface. This can also be observed from the peaks of the X-ray diffractogram as seen from Fig. 4, in which X-ray diffraction of the laser treated surface is shown. In the second layer, dendritic structure is formed because of relatively lower cooling rates than that of the surface. As the depth below the surface increases large grains are formed in the third region. The demarcation line is not observed at the interface of the treated layer and the base material. This is because of the high thermal conductivity of bronze, which causes high rate of heat conduction from the treated layer to the solid bulk while modifying the microstructure in the interface region.

Fig. 5 shows the results of Potentiodynamic polarization response of laser treated and untreated surfaces in 0.1 M NaCl solution at room temperature. It is clear from Fig. 5 that laser treated sample exhibits better corrosion resistance than the untreated specimen in terms of pitting potential (E_{pit}) and passive current density (i_p). Corrosion potential (E_{corr}) is found to be -400 mV > -120 mV for laser treated and untreated specimens, respectively. Laser treated specimen shows a pitting potential of 300 mV_{SCE} as compared to 70 mV_{SCE} for untreated specimen. Passive current density (i_p) as well as corrosion current (i_{corr}) density of laser treated specimen are much less than that of untreated specimen. All these results suggest that a stable and more protective film is formed on the laser treated specimen surface; therefore, laser treatment has a positive effect on the corrosion properties of bronze surface. Table 3 summarized the results of potentiodynamic polarization.

To confirm the potentiodynamic polarization data, the values of corrosion rate for two specimens are calculated using Tafel analysis. It is found that corrosion rate of laser treated specimen (0.00037 mpy) is much lower than that of untreated specimen (0.0083 mpy), which is in agreement the results shown in Fig. 5. Furthermore, electrochemical impedance spectroscopy (EIS) measurements are carried out at OCP, by applying a sinusoidal potential perturbation of 10 mV with frequency sweep from 100 kHz to 0.01 Hz. The findings are shown in Fig. 6; in which case, it can be observed that polarization resistance value (R_p) of laser treated specimen is much higher than that of untreated specimen, suggesting that it has higher corrosion resistance. The large semicircle of laser treated specimen corresponds to higher corrosion resistance behavior than untreated specimen. These results show the positive effect of laser treatment on the corrosion properties of bronze.

Fig. 7 shows SEM micrographs of pit sites at the laser treated and as-received workpiece surfaces. It is evident from the SEM micrographs that pit site is smaller and shallow for laser treated surface as compared to corresponding to as-received surface. Consequently, laser treated layer acts as a passive layer lowering the surface pitting during the electrochemical testing. The pits formed at the surface do not have a regular pattern and the secondary pitting in the pit sites is not observed for both laser treated and as received surfaces.

4. Conclusion

Electrochemical response of laser treated bronze surface is investigated in aqueous solution. Morphological and metallurgical changes in the laser treated layer are examined using the analytical tools. Pit sites at the surfaces are analyzed incorporating scanning electron microscope. It is found that laser treated surface is free from asperities such as cavities, voids, and micro-cracks. The overlapping of the laser irradiated spots along the laser scanning tracks do not contribute significantly to the surface roughness. Laser treated layer extends uniformly below the surface with a thickness in the order of 40 μm. The close examination of the cross-sections of the treated layer reveals that fine grains in a dense layer are formed in the surface region. This is attributed to the high cooling rates at the surface. The presence of Cu_3N nitrides is evident from the X-ray diffractogram, which contributes to the formation of the dense layer at the surface due to the volume shrinkage. Dendritic structure is formed below the surface due to relatively slower cooling rates as compared to that at the surface. Large grains are observed in the heat affected zone region. The corrosion current density for the laser treated surface is much less than that of the as-received surface indicating the laser treatment provides protective layer at the surface. This finding is also supported by the electrochemical impedance spectroscopy results. The pits sites on the laser treated surface appear to be shallower and smaller in size than that corresponding to the as-received surface. The close examination of the pit sites revealed that no secondary pitting takes place at the laser treated and untreated surfaces.

Acknowledgements

The authors acknowledge the support of Deanship of Scientific Research, King Fahd University of Petroleum and Minerals, Dhahran, Saudi for supporting the funded project # SB111003.

References

[1] J-L. Xu, B. Yang, W. Gao, Z.-P. Wang, D.-W. Long, C.-Y. Ju, T. Yu, J Aeronautical Mater. 29 (1) (2009) 63–67.
[2] A. Gisario, D. Bellisario, F. Veniali, Int. J. Mater. Form. 3 (1) (2010) 1067–1070.
[3] C.H. Tang, F.T. Cheng, H.C. Man, Surf. Coat. Technol. 200 (8) (2006) 2594–2601.

[4] C.T. Kwok, P.K. Wong, W.K. Chan, F.T. Cheng, H.C. Man, in: 29th International Congress on Applications of Lasers and Electro-Optics, September 26–30, 2010, ICALEO 2010 – Congress Proceedings, vol. 103, 2010, pp. 1518–1524.
[5] R.D. Klassen, C.V. Hyatt, P.R. Roberge, Can. Metall. Q. 39 (2) (2000) 235–246.
[6] A.N. Mazurkevich, I.N. Shiganov, R.S. Tretyakov, O.Y. Elagina, A.K. Prygaev, A.V. Buryakin, Y.V. Baklanova, Chem. Pet. Eng. 48 (5–6) (2012) 380–383.
[7] H. Garbacz, E. Fortuna-Zalesna, J. Marczak, A. Koss, A. Zatorska, G.Z. Zukowska, T. Onyszczuk, K. Kurzydlowski, Appl. Surf. Sci. 257 (17) (2011) 7369–7374.
[8] T. Kawazoe, A. Ura, M. Saito, S. Nishikido, Surf. Eng. 13 (1) (1997) 37–40.
[9] S. Kac, A. Radziszewska, J. Kusinski, Appl. Surf. Sci. 253 (19) (2007) 7895–7898.
[10] B.S. Yilbas, A. Matthews, A. Leyland, C. Karatas, S.S. Akhtar, B.J. Abdul Aleem, Appl. Surf. Sci. 263 (2012) 804–809.
[11] B.S. Yilbas, S.S. Akhtar, C. Karatas, Int. J. Adv. Manuf. Technol. (2012) 1–13.
[12] B.S. Yilbas, S.S. Akhtar, C. Karatas, C. Chatwin, Surf. Interface Anal. 44 (2012) 831–836.